16th World Conference on Earthquake, 16WCEE 2017
Santiago Chile, January 9th to 13th 2017
Paper N° 1006

UNUSUAL FINDINGS AFTER THE 2015 NEPAL GORKHA M 7.8 EARTHQUAKE FROM ENGINEERING AND GEOLOGICAL POINTS OF VIEW

P. Carydis[(1)], E. Lekkas[(2)], I. Taflampas[(3)], E. Skourtsos[(4)], S. Markantonis[(5)], S. Mavroulis[(6)]

[(1)] *Professor of Earthquake Engineering, Professor Emeritus of the National Technical University of Athens, Greece, Member of the European Academy of Sciences and Arts, Panagouli 5a str., Kifissia, Greece, e-mail: pkary@tee.gr (corresponding author)*
[(2)] *Professor of Dynamic Tectonic Applied Geology, Department of Dynamic, Tectonic and Applied Geology, Faculty of Geology and Geoenvironment, School of Sciences, National and Kapodistrian University of Athens, Greece, e-mail: elekkas@geol.uoa.gr*
[(3)] *Civil Engineer Phd, Laboratory Teaching Staff, Laboratory of Earthquake Engineering National Technical University of Athens, Greece, e-mail: taflan@central.ntua.gr*
[(4)] *Geologist Phd, Laboratory Teaching Staff, Department of Dynamic, Tectonic and Applied Geology, Faculty of Geology and Geoenvironment, School of Sciences, National and Kapodistrian University of Athens, Greece, e-mail: eskourt@geol.uoa.gr*
[(5)] *Civil Engineer MSc, e-mail: markantona@yahoo.gr*
[(6)] *Geologist MSc, PhD Candidate, Department of Dynamic Tectonic Applied Geology, Faculty of Geology and Geoenvironment, School of Sciences, National and Kapodistrian University of Athens, Greece, e-mail: smavroulis@geol.uoa.gr*

Abstract

Despite the large magnitude and the shallow depth of the 2015 Nepal earthquake, no consistent surface rupture was observed, except from a highly disrupted zone in Araniko Highway probably attributed to thrust faulting directly located under the Kathmandu basin. Kathmandu city is situated at about 76 km to the ESE of the epicenter of the main shock. This distance, in general, might be considered as rather long, but the observed disrupted zone may be due to the very small northward dip of the fault combined with the hypocenter depth and location.

The incurred structural damage was extended over a rather large area along the main axis of the country. The damage intensity varied strongly over a vast region, even among adjacent structures. On the other hand, attenuation of the damage intensity as a function of the epicentral distance up to around 80 km was not observed. Field observations included cases of negligible to slight damage as well as cases of heavy damage to destruction. Intermediate level of damage was not observed. Most buildings were constructed with fired clay brick masonry and wooden roofs and floors. In these cases, the observed damage started from the roof and the top floors. In case of collapse, debris was distributed symmetrically around the vertical axis of the building. This type of structural response implied that the structures have been excited dominantly along the vertical direction. In some cases, intermediate floors have been crushed. Window glass panels were not broken in the intact parts of the almost all partially collapsed buildings. These phenomena can be explained by considering not only the structural characteristics and deficiencies, but also the convolution of different types of emerging seismic waves. Despite the inadequate aseismic design, the great height and the flexibility of the majority of the reinforced concrete buildings, they performed well during the earthquake.

The ground motion was characterized by low ground accelerations due to filtering of the deep soil deposits of the site as well as large velocity pulses with periods over 4 sec caused by directivity effects. These directivity effecs occurred because the rupture was directed towards Kathmandu, but they had no effect on structures since they presented very low frequency content. The recorded ground motion was dominated by predictable values of frequency and amplitude due to the source mechanism of the event.

Keywords: Nepal 2015 earthquake; geoscientific findings; vertical earthquake component; forward directivity

1. INTRODUCTION

A violent earthquake of magnitude M 7.8 hit Nepal on Saturday April 25th, 2015 at 06:11 UTC (11:56 local time) (Fig. 1a). The shake has been felt all over Nepal, India, Tibet and Bangladesh and caused major damage in Kathmandu and its surroundings including a number of centuries-old temples. The death toll exceeds 8000 victims. The earthquake also triggered avalanches on Mount Everest, which killed at least 17 people at the base camp.

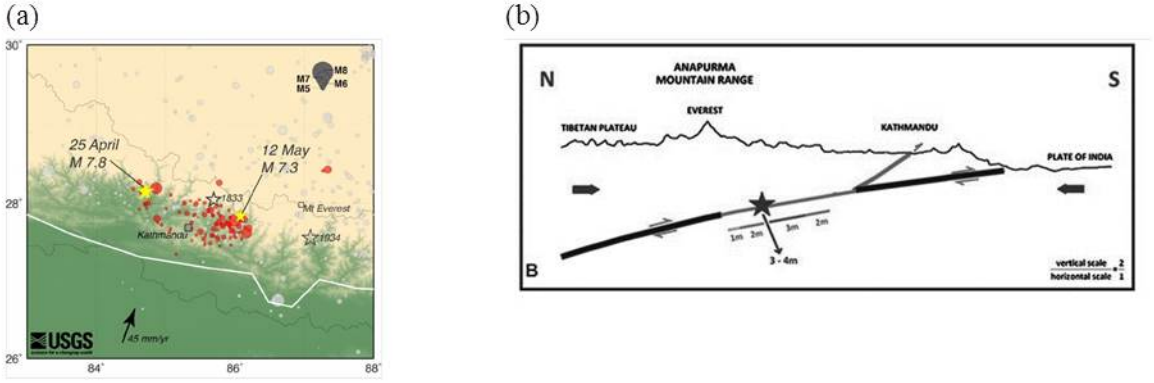

Fig. 1 – (a) Main events and aftershock locations of 2015 central Nepal earthquake sequence (USGS, 2015). (b) Sketch showing the proposed model of the fault geometry ruptured during the 2015 central Nepal earthquake. The star indicates the earthquake hypocenter. Thinner line indicates the ruptured segment of the Main Himalayan Thrust (MHT), while the thicker line indicates segments that were not activated. The rupture was propagated southwards and eastwards along the MHT and then upwards along a thrust fault that is linked to the MHT. The surficial trace of that fault was observed at the SE suburbs of Kathmandu city.

The study team moved to Nepal immediately after the earthquake and visited earthquake stricken sites that were accessible by car, for five days, over a region covering around 60 km to the north-west and around 40 km to the south-east of Kathmandu city. In this paper, the most significant observations are presented in order to explain the incurred damage. A commentary on societal aspects, on disaster management and on emergency response and involvement of the international community is presented, based on the on-site experience of members of the study team which arrived in the affected area immediately after the earthquake and conducted field survey during the critical period of the first five days following the disaster.

The region belongs to the Himalaya Arc, which is frequently affected by major earthquakes with Mw 7.5 or more [1, 2, 3]. The Himalaya orogen is the result of the collision of India and Eurasia that started during the latest Paleocene to early Eocene and the subsequent northward subduction of India [4, 5]. Major Cenozoic normal or thrust faults with a general northward dip are observed in the Himalaya thrust belt: the Main Frontal Thrust (MFT), the Main Boundary Thrust (MBT), the Main Central Thrust (MCT) and the South Tibetan Detachment System (STDS) [6 and references therein]. All thrust structures can be observed throughout the mountain chain and it is suggested that they are linked to a large-scale detachment, the Main Himalayan Thrust (MHT).

2. SEISMOLOGICAL DATA AND DEFORMATION ZONES

The earthquake epicenter of the April 25, 2015 event was located near the village of Barpak in Gorkha district (28.147°N and 84.708°E), which was completely destroyed by the earthquake. Based on USGS, the earthquake was assessed as Mw 7.8. Its focal depth was only 11-15 km; the activated thrust fault had a WNW-ESE strike

with 7º-10º dip towards the north [7]. Seismological data and a crustal-scale geological section, suggest that the earthquake has ruptured a segment of the Main Himalayan Thrust (MHT). The rupture started at the epicenter and propagated eastward for about 130 km, rupturing the area directly under the Kathmandu basin (Fig. 1b).

A wide ground deformation zone associated with thrust faulting was observed at the southeastern suburbs of Kathmandu city and was characterized by the formation of monocline-like escarpments with height ranging from 0.5m to 1.8m (Fig. 2). Deformation in the hanging wall of the thrust was also detected. Tension cracks and small-amplitude folds were also observed (Fig. 2a-c).

Fig. 2 – (a) View of a spectacular ground crack of the central Nepal highly disrupted zone along the northern side of the Araniko Highway, Kathmandu city. The ground deformation comprised escarpments with height of about 1.6m. Tension cracks were formed at the crest of the zone. (b) Another view of ground cracks resulting in tilted bricks along the northern pavement of the Araniko Highway. The ground on the right (NNW) presented an uplift of about 1.3 m compared to the ground on the left (SSE). The crest of the escarpment was faulted and discontinuous. The initially flat pavement bricks and cement slab were tilted near the crest of the escarpment. (c) The concrete yard was fractured due to ground deformation and uplifted due to N-S compression. Note that the house remained intact. (d, e) Many multistoried buildings were tilted without structural damage.

This 1km long and 200m wide ENE-WSW striking highly disrupted zone runs diagonally to the Araniko Highway in Gatthaghar, SE of the National Airport. The northern area was uplifted about 1.0-1.8m compared to the southern area resulting in low monoclinal escarpments (Fig. 2a-b). The deformation zone in the asphalt road presents tensional cracks with a width of 15-60cm and a vertical throw of 20-40 cm. The above mentioned ground cracks are in agreement with preliminary models of co-seismic slip which suggest that the largest amount of slip on the fault was located just below the city of Kathmandu.

Many buildings along this highly disrupted zone were tilted as solid bodies. However, it is significant to note that damage due to structural response was not observed (Fig. 2d-e). Moreover, the ground deformation along the highly disrupted zone caused damage or even destruction of small constructions such as walls and pavements in the house yards leaving unaffected the buildings (Fig. 2c).

3. SEISMIC RESPONSE OF STRUCTURES

The scope of this section is mainly to discuss the response of the various structures and secondarily to infer some basic characteristics of the respective ground motion. The latter one can be determined from a detailed observation of the seismic response of a structure.

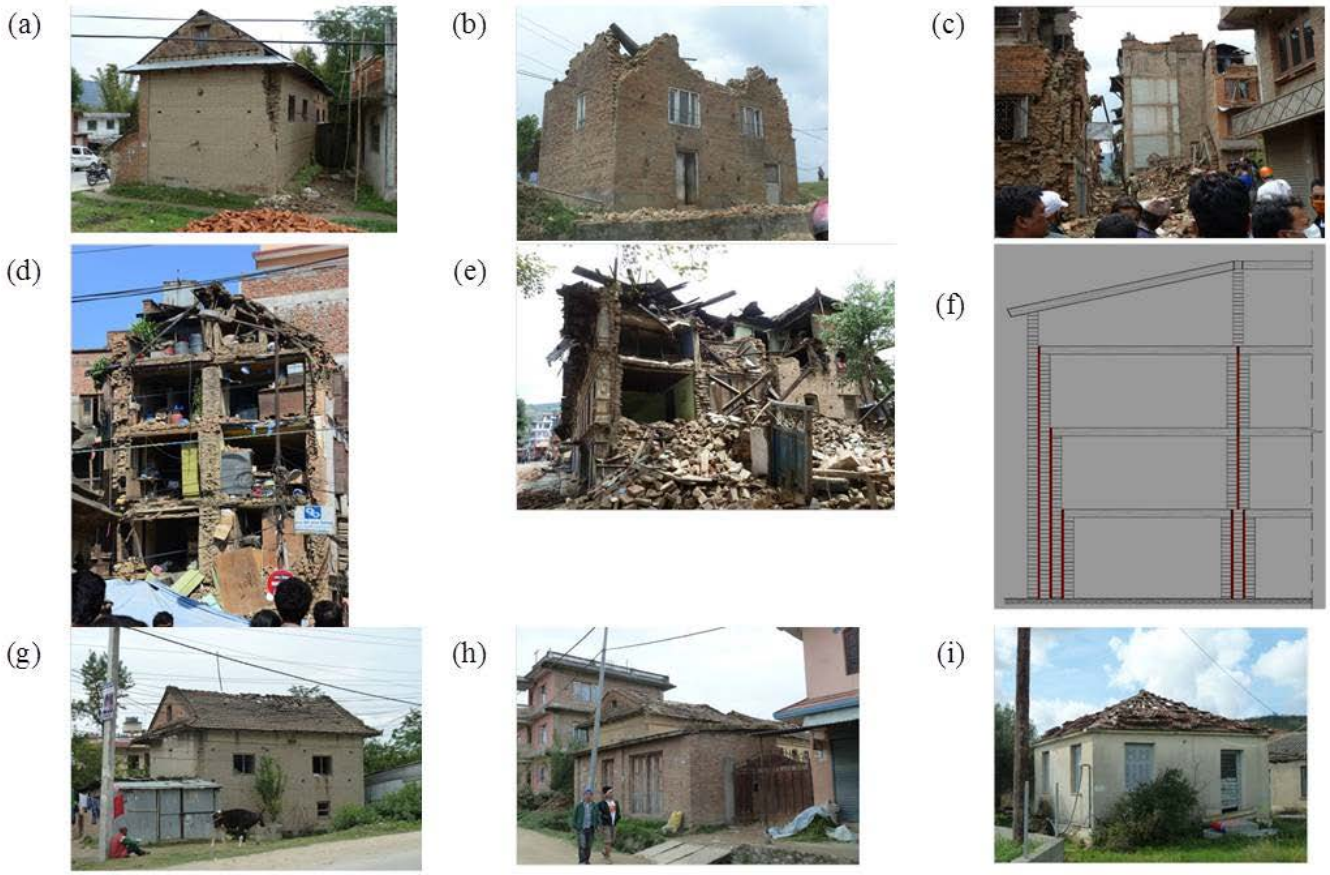

Fig. 3 – Representative seismic response of buildings during the 2015 Nepal earthquake. (a) The upper parts of the four corners have symmetrically fallen vertically. (b) In addition to (a), the damage was initiated from the rooftop, the window glass panels remained intact, debris was spread symmetrically around the building. (c) Recently constructed buildings have common walls with the adjacent older ones and, generally, the walls of the recently constructed buildings are free-standing vertical cantilevers. (d) The content of severely damaged buildings, as well as free standing objects, presented slight movement. (e), (f) Vertical layers of the walls are built without any connection between them. (g), (h) Roof tiles have been dislocated symmetrically to the roof tree. Similar damage was induced by the 2014 Cephalonia (Ionian Sea, Western Greece) earthquakes (Mw 6.0) (i).

It must be emphasized that the response of the various types of structures mentioned below is almost identical and independent of their location, unless stated separately.

The response of monumental structures was very poor in spite of the low ground accelerations. It was observed that these structures are constructed with solid fired clay bricks without mortar or with an earthen one. This mortar did not possess any bond with the bricks. The response of a great number of traditional structures was equally very poor despite the fact that a considerable number of such buildings with poor workmanship withstood the earthquake without any damage. These structures are up to four and in some cases five levels high including the roof. Almost all horizontal load-bearing elements (roofs, floors and lintels) are from timber. In some cases the timber floors and lintels are strengthened with steel beams. The floor beams penetrating the walls are functioned as levers in the vertical direction against the stability of the above standing wall. This is especially pronounced during a vertical excitation of the floor.

In general, the walls are 50 – 70 cm thick and are composed of vertical brick layers which are not always transversely connected, as it is shown in Fig. 3a,b,e,f. Thus, the masonry is quite vulnerable to horizontal and vertical ground excitations. In severely damaged buildings, these independent and rather thin walls buckled vertically. Transverse walls are not structurally and solid connected and the walls are freely standing. Ties

through the roof were ineffective. Cracks were horizontal or vertical, limited in density, length and thickness. Diagonal cracks were not observed. In many cases, damage was caused by the vertical impact of the roof on the walls. Another noticeable characteristic of the response of this type of buildings was the absence of any horizontal relative motion or impact between adjacent buildings or any significant damage on the secondary elements. There was no displacement of the free standing objects inside and outside the buildings, as it is shown in Fig. 3. In buildings with negligible to slight damage, the roof tiles were symmetrically dislocated starting from the roof tree. This type of damage was also observed during the 2014 Cephalonia (Ionian Sea, Western Greece) earthquakes as it is shown in Fig. 3g, h, i.

The symmetrical damage of masonry buildings around the vertical axis, with the top parts of corners shaken off, forming a V shaped failure as shown in Fig. 3a and 3b, became a subject of a special investigation following a reverse analytical procedure. Namely, knowing the response of the structure we tried to define the excitation. The abovementioned type of failure is observed not only in numerous sites of Nepal after the recent event, but also in many other epicentral areas of previous destructive earthquakes around the world.

In order to investigate this type of failure, a simple masonry building 7.0 m x 7.0 m in plan, and 3.5 m height was selected as test model that was shaken with almost all probable types of ground excitations at a time (horizontal and vertical, natural and artificial earthquake time histories, half and full cycle pulse or harmonic excitations, combined with a variety of peak accelerations up to 1.5g). The criterion for the selection of the most probable ground excitation, was that the shape of the developing isostress lines in the walls of the model should be as close as possible to the observed V shaped failures. After numerous trials, the most probable ground excitation proved to be that of a half cycle vertical pulse with an acceleration that exceeds 1.0g. The response of the model was not sensitive to the duration of the half cycle pulse.

(a) (b) (c)

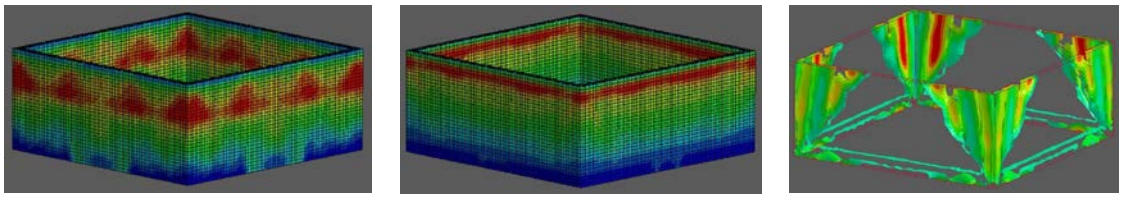

Fig. 4 – (a, b, c) A simple in plan 7.0 m x 7.0 m and 3.5 m height roofless masonry house, under a vertical strong impact motion gave isostress lines identical to those observed at numerous sites (compare with damage pattern of Fig. 3 a,b).

Contemporary buildings can be divided in two groups. The first includes buildings before 1996, when the first building code of Nepal was implemented. These buildings are less than 7 – 8 stories high. Generally, their load-bearing system comprises reinforced concrete filled with solid fired clay brick walls. The dimensions of the concrete elements are very small, remaining constant along the height of the building. For example, the central columns of a 5-6-storey building are 0.25 m x 0.25 m ÷ 0.30 m x 0.30 m at distances of 4 – 5 m. Generally, the quality of concrete and the workmanship is poor. The reinforcement is sparse and small in diameter. Shear walls were not used. Their flexibility is augmented due to soft soil conditions, small plan dimensions and many stories.

As it is shown in Fig. 5, two types of response of these buildings are clearly distinguished: In the first type (Fig.5d, e, g, h), which covers the majority of the buildings, no damage was observed, the glass panels remained intact and no horizontal motion or impact was detected. This observation is quite interesting since the resulting horizontal motions were null in spite of the quite unfavorable combination of a high magnitude earthquake, at an epicentral distance of 30 – 80 km, of rather deep soft soil conditions and flexible multistoried buildings. The same is observed in the category of traditional and stiffer structures. In the second type, which covers a very small number of buildings, total or partial collapse was observed. The collapse was within the plan of the building in a pancake mode (Fig. 5a). The failure mode could be found at three different locations, as it is schematically shown in Fig. 5b, at the ground floor, at the intermediate level, or at the top level. The same mode of failure was also observed in the previous category of traditional buildings.

Fig. 5 – Representative seismic response of buildings during the 2015 Nepal earthquake. (a) Contemporary buildings with a crushed ground or intermediate floor. (b) Damage may occur at any point along the height of the structure depending on the point of interference of incident and reflecting vertically propagated seismic waves. (c, d, e, f, g) No relative motion observed between adjacent buildings of any type and site. (f) A close-up of the adjacent upper parts of the buildings shown in the picture (e). (h) and (i) Two flexible contemporary adjacent 8-storey buildings possess a common and untied point at their top, which has not been cracked, unlike the quite commonly anticipated impact or at least detachment after earthquakes.

Buildings constructed after 1996 according to the national anti-seismic code are much safer. Those buildings have a height of up to 20 storeys, are stiffer and of sounder design and construction quality. Nevertheless, even this category of buildings appears to have suffered damage shown in Fig. 5a.

During our field survey, we also investigated infrastructures, for example a rather long span suspended bridge, an arched bridge, several other smaller bridges and retaining walls along the road, and observed no damage, displacement or dislocation except at the pedestrian bridge and relevant infrastructures that were adjacent to the highly disrupter zone described in the previous chapter.

4. CHARACTERISTICS OF THE KANTI PATH RECORD OF THE 2015 NEPAL GORKHA EARTHQUAKE

Near-fault ground motions are affected by directivity phenomena, which produce important velocity pulses, mostly associated with the normal to the fault direction. Directivity pulses amplify the long period coherent component of the ground motions and are explicitly apparent in the velocity and the displacement time histories and the related response spectra. A number of methods are commonly used for the identification of the parameters of the velocity pulses, mainly their period and amplitude. Also, several mathematical expressions have been proposed for their mathematical representation, which vary from simple functions to more complicated wavelets.

A very efficient wavelet is the one proposed by Mavroeidis and Papageorgiou (M&P) [10], which, beyond the period and the amplitude, uses additional parameters related to the total duration and the phase shift of the pulse. In this paper, a recently proposed new method [11] is used, which allows the explicit determination of the parameters of the pulse contained in pulse-like records. The M&P wavelet is used for the mathematical representation of the pulse. First, the period of the pulse is determined from the peak of the $S_d \times S_v$ *product spectrum*, a new concept defined as the product of the velocity and the displacement response spectra. The remaining parameters of the M&P wavelets are derived from the targeted response spectrum of the ground motion, using an iterative procedure and defining subsequent wavelets from the residual ground motion after each iterative cycle. The method follows a well-defined procedure easily implemented in a computer code for the automatic determination of the pulse parameters of a given ground motion. The proposed method can be extended to the determination of additional pulses inherent in the ground motion. To this end, the detected significant pulse is subtracted from the original record to derive the *residual record*, to which the method is applied for the derivation of the second pulse. This procedure can be repeated several times until all significant pulses are derived. The summation of all significant pulses produces a very accurate mathematical representation of the original record.

In the case of the Kanti Path record a sequence of six pulses has been determined in order to define the velocity time history and the relevant spectra. As seen in Fig. 6a, the approximation of the velocity time history with the six pulses is almost perfect. The same is observed for the relevant velocity spectra (Fig. 6b). The main characteristics of the record are its low acceleration values, close to 0.15g as shown in Fig. 7a, b, which may be due to the soil deposit filtering at the recording site, where the V_s30 is approximately 200 m/sec [8]. The other characteristic of the strong ground motion is the directivity effect, pronounced in the two horizontal components, where strong velocity pulses with period around 5.0 sec and amplitude of approximately 80 to 100 cm/sec are observed (Fig.7a, b). As far as the acceleration spectra are concerned, a bell-shaped amplification is observed (Fig.7c, d), in agreement with [9], around the pulse period, which is also the predominant period of the acceleration spectrum for the east component of the record.

The velocity spectra of both Kanti Path components present a predominant period around 5.0 sec, which is close to the pulse period. An analysis performed according to the method of [11], in order to evaluate the M&P [10] wavelets that can mathematically simulate the velocity time history, showed that the east component of the record includes an M&P wavelet with a period of 4.99 sec, amplitude of 93.21 cm/sec and a large number of pulse cycles. The cross correlation coefficient between the original velocity time history and the extracted wavelet is 90% presenting a very good fitting. The north component includes a wavelet with a period of 5.39 sec and amplitude of 87.87 cm/sec. The cross correlation between the original velocity time history and the extracted wavelet is 83%. The two horizontal velocity time histories are closely correlated with a coefficient of 76%. The period of the directivity pulses is, as well known, exponentially related to the event moment magnitude and in this case close to the predicted values.

The maximum ground velocity values for the two horizontal components are about two thirds of the mean value of the expected fault slip velocity which is about 150 cm/sec and are a good estimate for directivity pulse amplitudes near large ruptured asperities. A case with similar ground velocity, filtered high frequency non-coherent component of the ground motion due to the soil deposit, and a pulse period quite smaller and equal to 1.49 sec, was observed during the 2014 Cephalonia earthquake [12]. In this case the correlation coefficient

between the first dominant pulse and the original record was 88%, an also very good fitting. At the recording site the V_s30 is approximately 270 m/sec. As it is observed from these two records, the pulse period is a function of the moment magnitude of each event, but the maximum ground and spectral velocities are similar close to the maximum up to now observed values and not affected from the event magnitude. These observations are consistent with those referred in [10].

The most significant point in both cases is that the non-coherent high frequency component of the ground motion is almost absent (possibly due to soil filtering) and the coherent low frequency part is dominated by the directivity pulse, which is predominant even in the acceleration time history. In both cases, the acceleration of the extracted wavelet is equal to the acceleration of the original record (0.15g for the 2015 Nepal Gorkha earthquake and 0.6g for the 2014 Cephalonia earthquake) if we consider that the maximum pulse acceleration is equal to the product of the maximum pulse velocity with the circular pulse frequency.

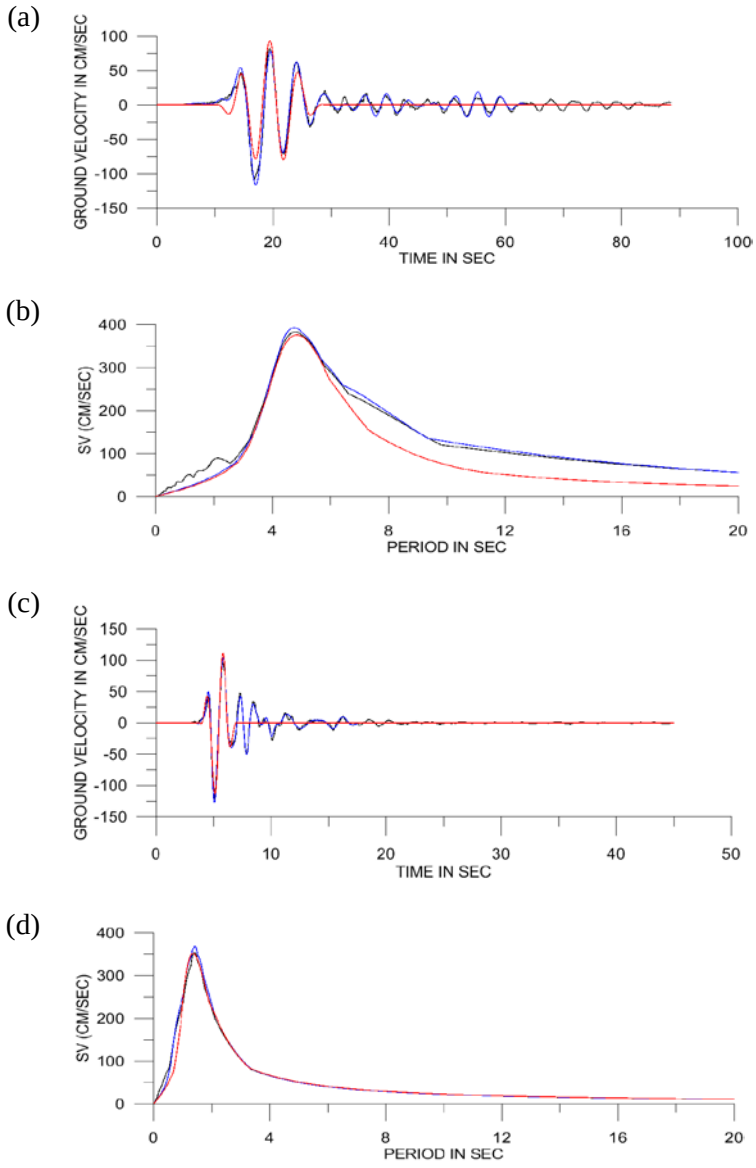

Fig. 6 – (a) The velocity time history of the eastern component of the Kanti Path record is presented, where the original time history is given in black, the combination of six pulses in blue and the first dominant pulse in red. (b) the relevant velocity spectra are given with the same colour identification. (c, d) The velocity time history and the velocity spectra are given for the Lixouri eastern component of the Cephalonia 2014 earthquake respectively.

As a result the peak spectral accelerations are estimated at the pulse period and the shape of the acceleration spectrum is different from the usual one taken into account in the regulations.

Furthermore, the ductility demand was calculated for Ry=3. Here again the effect of the directivity is also evident. In agreement with the observation made in [13], the ductility values are quite larger than the reduction factor at a period range lower than half the pulse period (Fig. 8a, b).

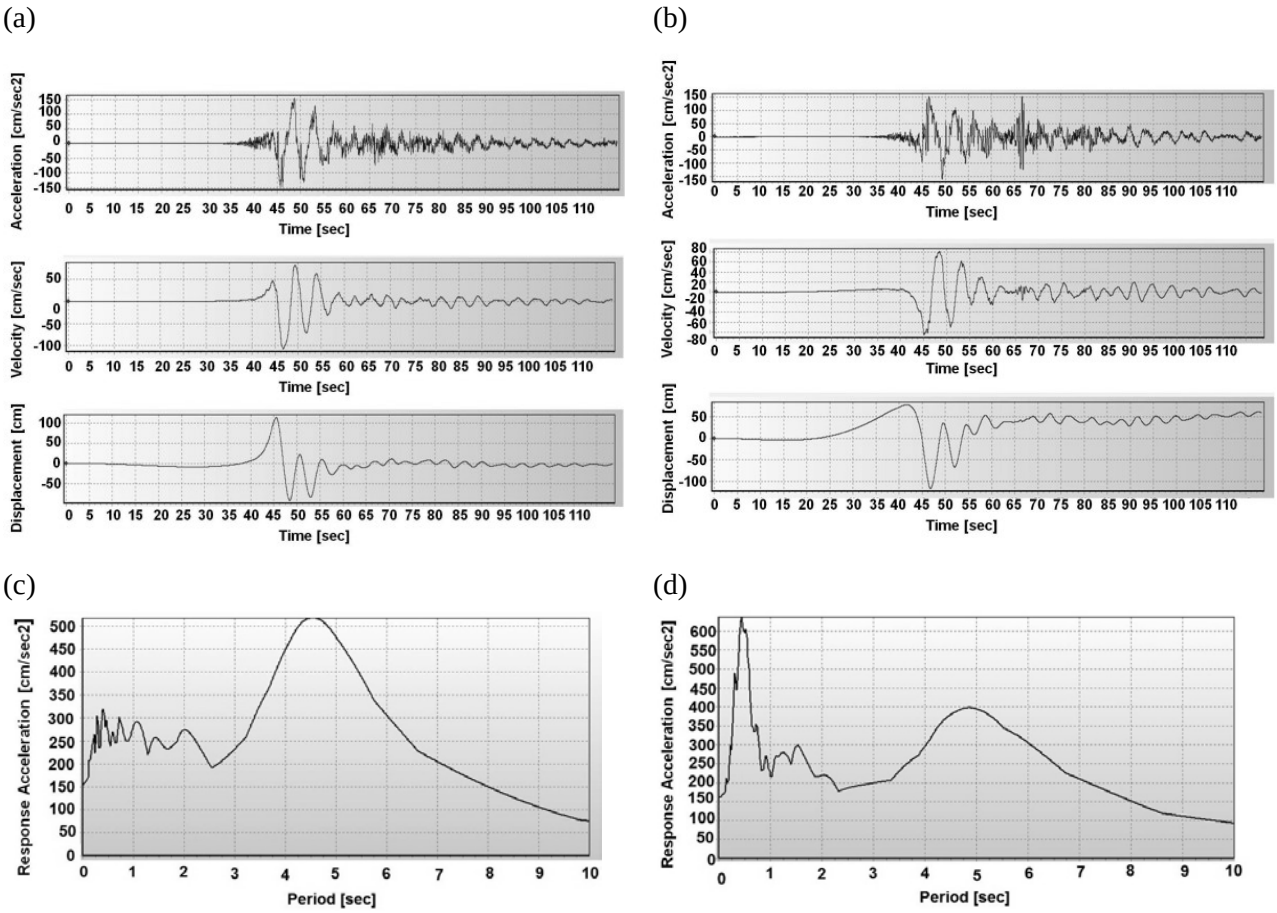

Fig. 7 – Ground motion time histories for Kanti Path record (a) East component (b) North component. (c), (d) Acceleration response spectra.

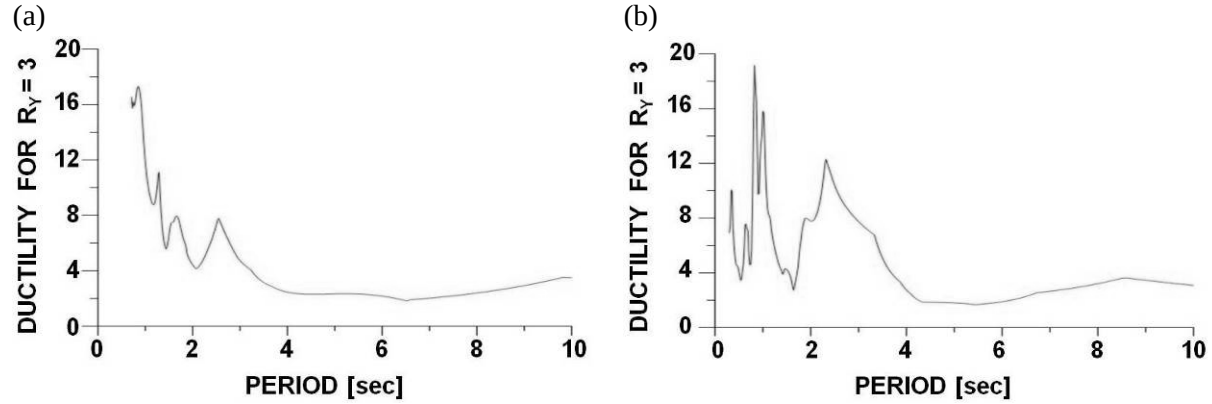

Fig. 8 – Ductility for Ry=3 in (a) and (b) for the east and north ground motion components respectively.

From the presented records, it can be inferred that, in case of quite soft soil deposits, the non-coherent, high frequency part of the ground motion is filtered and the coherent, low frequency, pulse-like part is predominant. The characteristics of the pulse –like part of the motion depend on the source mechanism of the seismic event and can be estimated. The period of the pulse has been found to be exponentially associated to the moment magnitude of the event and the pulse amplitude, close to the peak ground velocity, is associated to the slip rate of the adjacent fault asperities. As a result, ground motions, on soft soil deposits, affected by near-source directivity effects are quite predictable.

5. CONCLUSIONS

The April 25, 2015 Nepal earthquake caused a wide ground deformation zone associated with thrust faulting and more specifically the formation of monocline–like escarpments associated with tension cracks and small-amplitude folds, confirming the early models of co-seismic slip which suggest that the largest amount of slip on the fault was located just below the Kathmandu city.

The seismic intensity in the broader epicentral area was comparatively low. Monumental and traditional buildings suffered the most damage due to inadequate construction and maintenance. In case of sounder construction, buildings remained intact.

The majority of contemporary buildings with a reinforced concrete load-bearing system and brick infill and partition walls withstood the earthquake without damage despite the fact that most of them were seismically vulnerable. Other structures as bridges, retaining walls etc. did not present noticeable damage.

Relative lateral motion between adjacent buildings was not detected in numerous cases all over the affected area. There was observed either partial or total collapse of buildings or lack of horizontal motion, vertical or horizontal cracks and no damage to glass window panels. Diagonal cracks were not detected. This observation is a key characteristic of the predominance of vertical component of the earthquake ground motion in the epicentral region and of the respective response of structures. In other words, epicentral region's characteristics were unusually quite extended in this event.

In agreement with the abovementioned findings, we defined a type of ground motion compatible with the observed pattern of structural response following a reverse analytical procedure. This type of ground motion contains a half cycle vertical pulse with a peak acceleration exceeding 1.0g.

The Kanti-Path record presents a coherent low frequency content dominated by directivity with an insignificant non-coherent high frequency component. This phenomenon appears characteristic if there is a combination of soft soil deposits with directivity affected ground motion, near large slip areas, as in the 2014 Cephalonia (Ionian Sea, Western Greece) earthquake with Mw 6.0. The difference in pulse period in each case is due to the event magnitude and is related to the relevant rise time and radius of the ruptured asperities. A further characteristic of both records is the similar ground velocity amplitude close to the mean value of the asperity slip velocity, considered about 150 cm/sec. It is possible that such values are representative of an upper level of directivity affected peak ground velocities, close to large asperities, independent of the moment magnitude. The recorded ground motion is defined by the source mechanism characteristics which are prevalent in the low frequency, pulse-like, content due to near-source directivity.

The authors consider that there are still items that deserve time and research efforts to be clarified and widely accepted.

7. REFERENCES

[1] Bilham R (2004): Earthquakes in India and the Himalaya: tectonics, geodesy and history, *Annals of Geophysics* **47** 839-858.

[2] Bilham R (2009). The seismic future of cities, *Bulletin of Earthquake Engineering*, **7**, 839-887.

[3] Bilham R, Gaur VK, Molnar P (2001): Himalayan seismic hazard, *Science*, **293**, 1442–1444.

[4] Hodges, K.V. (2000). Tectonics of the Himalaya and southern Tibet from two perspectives, *Bulletin of the Geological Society of America*, **112**, 324-350.

[5] Avouac J-P, Ayoub F, Leprince S, Konca O, van Helmberger D (2006): The 2005, Mw 7.6 Kashmir earthquake: Sub-pixel correlation of ASTER images and seismic waveforms analysis. *Earth and Planetary Science Letters*, **249**, 514-528.

[6] Chamlagain D, Gautam D (2015): Seismic hazard in the Himalayan intermontane basins: an example from Kathmandu Valley, Nepal. In: Shaw R, Nibanupudi HK (eds) Mountain hazards and disaster risk reduction. Springer, Japan, pp. 73-103.

[7] USGS United States Geological Survey (2015): M7.8 - 34 km ESE of Lamjung, Nepal. http://earthquake.usgs.gov/earthquakes/eventpage/us20002926

[8] Paudyal YR, Yatabe R, Bhandary NP, Dahal RK (2012): A study of local amplification effect of soil layers on ground motion in the Kathmandu Valley using microtremor analysis. *Earthquake Engineering and Engineering Vibration*, **11**, 257-268.

[9] Shahi SK, Baker JW (2011): An empirically calibrated framework for including the effects of near-fault directivity in probabilistic seismic hazard analysis. *Bulletin of the Seismological Society of America*, **101**, 742-755.

[10] Mavroeides GP, Papageorgiou AS (2003): A mathematical representation of near-fault ground motions. *Bulletin of the Seismological Society of America*, **93**, 1099-1131.

[11] Mimoglou PP, Psycharis IN, Taflampas IM (2014): Explicit determination of the pulse inherent in pulse-like ground motions. *Earthquake Engineering and Structural Dynamics*, **43**, 2261-2281.

[12] GEER Association Report (2014). 2014 Cephalonia, Greece Earthquakes. Report No. GEER-034

[13] Iervolino I, Cornell CA (2008): Probability of occurrence of velocity pulses in near-source ground motions. *Bulletin of the Seismological Society of America*, **98**, 2262-2277.